Multi-Resonance Dual-Polarised Symmetrically Cross-Slotted Square Patch Antenna for 5G Millimeter-Wave Broadband Applications

Qi Wu[1], Haipeng Yu[1], Yiming Yu[2], Songtao Gao[2], Chen Yu[1], and Haiming Wang[1]

[1]Southeast University
[2]China Mobile Group Design Institute Co Ltd

December 14, 2022

Abstract

A dual-polarized symmetrically cross-slotted square patch (SCSSP) antenna with multimode resonance is proposed for 5G millimeter-wave broadband applications. A symmetrical cross-slot is etched on the square patch surface to change the original E-field distribution where a whole square patch is cut into four disconnected equal parts. For both polarizations, this etching also tunes the resonance frequencies of the two modes to be sufficiently close to each other. Therefore, the antenna can realize good impedance performance within the wide designated bandwidth. Dual-polarized radiation of the SCSSP is vertically excited by three bow-tie-shaped slots and fed by two orthogonal substrate integrated coaxial lines. Simulated and measured results show that the fabricated prototype achieves a broad overlapped impedance bandwidth of 50.0% (24-40 GHz), isolation higher than 30 dB between the two input ports, stable radiation pattern, and low cross-polarization over the operating band. Moreover, the proposed SCSSP antenna with compact size, planar shape, and simple vertical feeding is very well-suited for two-dimensional array design.

Multi-Resonance Dual-Polarised Symmetrically Cross-Slotted Square Patch Antenna for 5G Millimeter-Wave Broadband Applications

Qi Wu,[1,2] Haipeng Yu,[1] Yiming Yu,[3] Songtao Gao,[3] Chen Yu,[1] and Haiming Wang[1,2]

[1] *State Key Laboratory of Millimeter Waves, Southeast University, Nanjing 210096, China*

[2] *Pervasive Communication Research Center, Purple Mountain Laboratories, Nanjing 211111, China*

[3] *China Mobile Group Design Institute Co., Ltd., Beijing 100080, China*

Email: hmwang@seu.edu.cn; chenyu@seu.edu.cn

A dual-polarised symmetrically cross-slotted square patch (SCSSP) antenna with multimode resonance is proposed for 5G millimeter-wave broadband applications. A symmetrical cross-slot is etched on the square patch surface to change the original E-field distribution where a whole square patch is cut into four disconnected equal parts. For both polarizations, this etching also tunes the resonance frequencies of the two modes to be sufficiently close to each other. Therefore, the antenna can realize good impedance performance within the wide designated bandwidth. Dual-polarised radiation of the SCSSP is vertically excited by three bow-tie-shaped slots and fed by two orthogonal substrate integrated coaxial lines. Simulated and measured results show that the fabricated prototype achieves a broad overlapped impedance bandwidth of 50.0% (24–40 GHz), isolation higher than 30 dB between the two input ports, stable radiation pattern, and low cross-polarisation over the operating band. Moreover, the proposed SCSSP antenna with compact size, planar shape, and simple vertical feeding is very well-suited for two-dimensional array design.

Introduction: In wireless mobile communications, the ever explosive growth of traffic demands more bandwidth to meet user requirements. The fifth-generation mobile communication system (5G) exploits the bandwidth resources in the millimeter-wave (mmWave) frequency bands of 26 GHz and 39 GHz [1, 2]. Apart from the bandwidth, polarisation diversity and multiplexing are another ways to improve data rate [3]. In terms of an mmWave antenna, the characteristics of broad bandwidth, dual polarizations, low profile, simple structure, and easy fabrication are crucial.

So far, diversified efforts have been utilized to broaden the mmWave antenna bandwidth. Some improvements were achieved by using new-fashioned structures, for example, a substrate-integrated waveguide (SIW) cavity-backed E-shaped patch antenna [4], a symmetrical E-shaped patch [5], cavity-backed slot antennas [6], magneto-electric (ME) dipoles [7], and stacked patch antennas [8]. Modifying the feeding structure can also improve the bandwidth. For example, the L-probe feeding [9] and the aperture coupled feeding [10] were used to excite the patch antennas to broaden the bandwidth. However, the above-mentioned antennas have only one linear polarisation. Recently, several kinds of dual-polarised antennas have been developed, such as aperture-coupled antennas [11, 12], cavity-backed slot antennas [13], ME dipoles [14], and stacked patch antennas [15]. Nevertheless, the bandwidths of these dual-polarised antennas are all less than 30.0%. In [16], a 42.5% bandwidth was achieved by dual-polarised ME dipole based on low-temperature cofired ceramic (LTCC) technology. Comparing with the print circuit board (PCB) process, the LTCC process is quite expensive, which limits its wide application. Furthermore, the antenna is hardly used for array design if its length or width is greater than half the free-space wavelength of center frequency.

In this study, a broadband dual-polarised cross-slotted square patch (SCSSP) antenna is presented. A piece of square patch is cut into four equal disconnected parts by two orthogonally placed slots where these two slots forms a cross-slot. For one linear polarisation, the longitudinal slot on the patch changes the E-field distribution of the TM_{20} mode to realize a broadside radiation pattern which has a small effect on the E-field distribution of the TM_{10} mode [5]. Likewise, the other orthogonal linear polarisation is realized using the TM_{02} and TM_{01} modes. Importantly, the transverse slot has little effect on the original current distribution of the TM_{10} and TM_{20} modes. Combining these four modes, two orthogonal linear polarizations with broad bandwidth are achieved. Moreover, two low-loss and ultra-wideband substrate-integrated coaxial lines (SICLs) are utilized to feed the antenna through three bow-tie shaped apertures. These two SICLs are orthogonal to each other and located in different layers. The multilayer printed circuit board process is used to fabricate the proposed antenna.

SCSSP Antenna:

Geometry: The configuration of the proposed SCSSP antenna is shown in Fig. 1(a). The antenna consists of four substrate layers with relative permittivity ε_r = 2.2 and their thickness is 0.508 mm, 0.508 mm, 0.254 mm, and 0.76 mm, sequentially from top to bottom. The antenna part is on the top of substrate 1, while the SICL feeding is integrated into substrate 2, substrate 3 and substrate 4. The four layers are bonded together using three bonding films of Rogers 4450 with thickness of 0.1 mm and ε_r = 3.4.

Detailed dimensions of the antenna are illustrated in Fig. 1(b). A square patch is etched by two orthogonal slots on the top of the substrate 1. This cross-slotted square patch is excited by two crossed apertures which are etched on the Ground 1. Aperture 1 is used to couple the signal from the Feedline 1, which can radiate the V-polarised radiation. The Feedline 1 is surrounded by metallic vias among substrates 2, substrates 3 and substrates 4, sandwiched by the Ground 1 and Ground 2, realizing the SICL 1. Aperture 2 etched on the Ground 1 and Aperture 3 etched on the Ground 2 are used to couple the signal from the Feedline 2. The Feedline 2 is surrounded by metallic vias, sandwiched by the

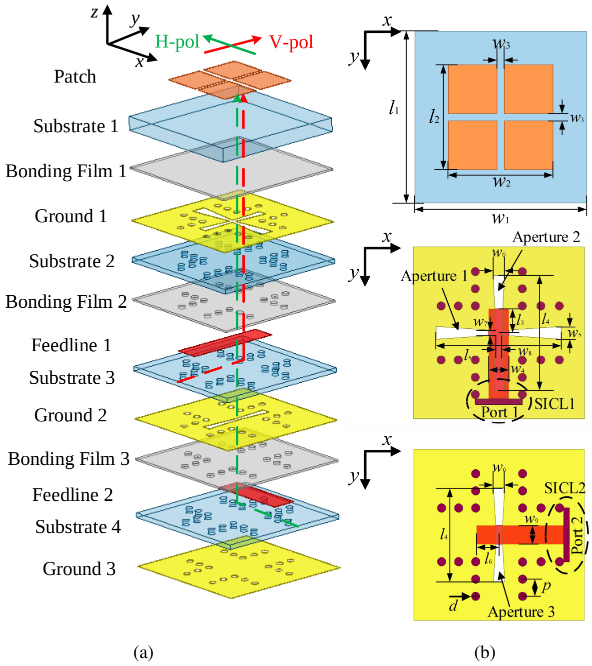

Fig 1 *Structure of the proposed dual-polarised SCSSP antenna. (a) Explosion view of the proposed antenna; (b) Top view of the cross-slotted square patch, Ground 1 with Feedline 1, and Ground 2 with Feedline 2.*

Table 1. Parameters of the proposed SCSSP antenna

Par.	Val. (mm)	Par.	Val. (mm)	Par.	Val. (mm)
l_1	6.00	w_1	6.00	w_7	0.15
l_2	3.58	w_2	3.58	w_8	0.23
l_3	1.05	w_3	0.25	w_9	0.55
l_4	4.30	w_4	0.65	d	0.30
l_5	3.50	w_5	0.41	p	0.60
l_6	0.85	w_6	0.32		

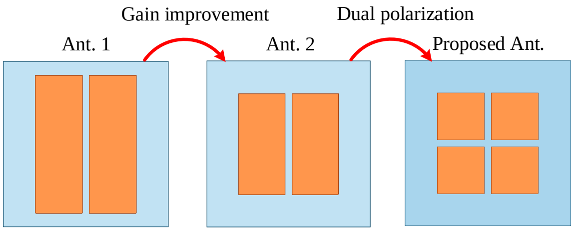

Fig 2 *Design procedure of the broadband dual-polarised patch antenna.*

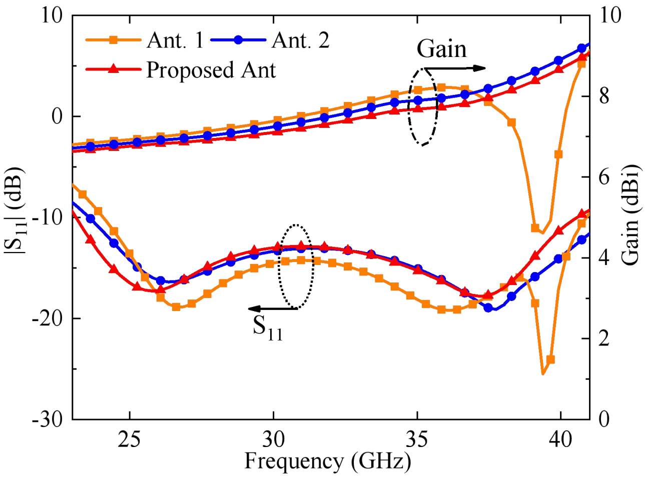

Fig 3 *Simulated reflection coefficients and gains of three kinds of antennas.*

Ground 2 and Ground 3, realizing the SICL 2. The parameters of the proposed antenna are illustrated in Table 1. The main design principle of the proposed patch antenna is summarized into three points, which are as follows.

1) The SICL feed and crossed slot are utilized to excite multiple TM modes of the dual-polarised antenna. Aperture 1 is used to excite TM_{10} and TM_{20} modes to radiate the V-polarised radiation. Apertures 2 and 3 are applied to excite TM_{01} and TM_{02} modes to generate the H-polarised radiation.
2) To remove the undesirable TM_{12} mode out of the operating band, the length of the patch is reduced to be equal to the width of the patch. Meanwhile, the symmetry between two orthogonal polarizations is achieved, which is important for dual-polarised antennas.
3) The shape of the coupled slots are changed into a bow-tie which can obtain wider impedance bandwidth [17]. In addition, the length of the bow-tie slot is shorter than the length of the rectangular slot which can reduce the size of the feed network.

Design Procedure and Analysis: Fig. 2 shows the design procedure of the proposed antenna. Ant. 1 and Ant. 2 are only fed by the SICL 1. The size of Ant. 1 is 5.0 mm × 3.58 mm, i.e., $0.53\lambda_0 \times 0.38\lambda_0$ where λ_0 is the free-space wavelength at center frequency. The longitudinal slot on Ant. 1 changes the E-field distribution of the TM_{20} mode. The TM_{10} and TM_{20} modes of Ant. 1 are used to construct a broadband linearly polarised antenna. The simulated reflection coefficient and gain of Ant. 1 are demonstrated in Fig. 3. It is seen that a wide impedance bandwidth of 50.0% (24–40 GHz) with $|S_{11}|$ less than -10 dB is achieved. However, the antenna gain has a sharp decrease around 39 GHz. It is mainly because a higher-order mode is excited around 39 GHz. With the help of the full-wave electromagnetic simulation tool Ansoft HFSS, the current distribution of Ant. 1 at 39 GHz is shown in Fig. 4(a), and it reflects the existence of higher-order mode resonance. The TM_{12} mode of the patch is excited around 39 GHz which results in the radiation pattern deterioration as shown in Fig. 4(b).

According to the cavity model theory of the patch antenna [18], the resonant frequency f_{mn} of each mode in the proposed SCSSP antenna

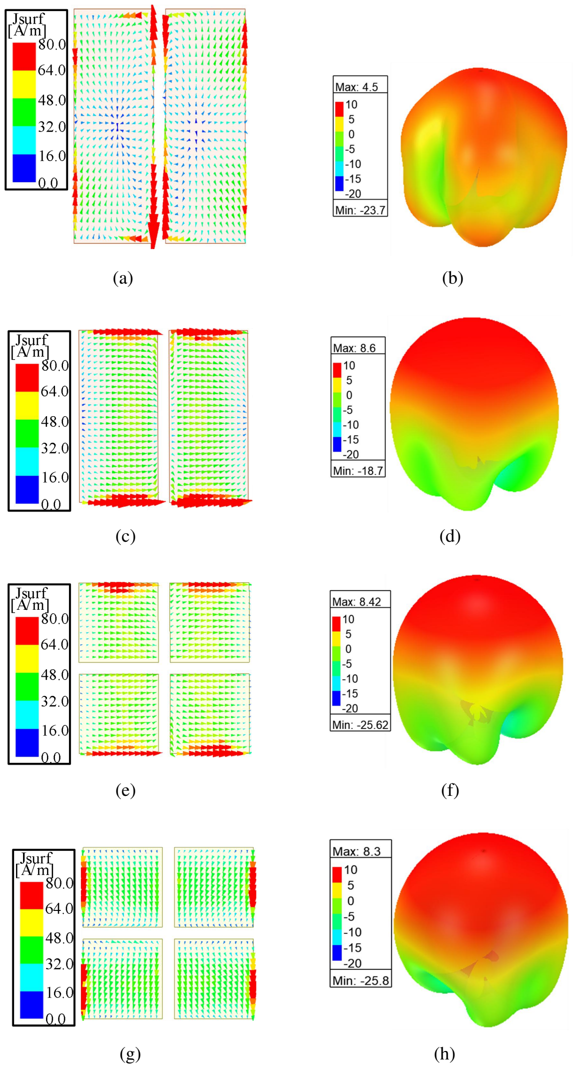

Fig 4 *(a) Current distribution and (b) radiation pattern of Ant. 1 at 39 GHz; (c) Current distribution and (d) radiation pattern of Ant. 2 at 39 GHz; (e) Current distribution and (f) radiation pattern of the proposed antenna at 39 GHz when port 1 is excited; (g) Current distribution and (h) radiation pattern of the proposed antenna at 39 GHz when port 2 is excited.*

can be determined by

$$f_{mn} = \frac{1}{2\pi\sqrt{\mu_r \varepsilon_r}} \sqrt{\left(\frac{m}{l_2}\right)^2 + \left(\frac{n}{w_2}\right)^2} \tag{1}$$

where m, n are integers, μ_r and ε_r are the permeability and the permittivity of Substrate 1, l_2 and w_2 are respectively the length and width of the patch. To overcome the unwanted higher-order mode resonance, two transverse slots are etched on the patch to suppress the TM_{12} mode in [5, 7]. As shown in Ant. 2 of Fig. 2, instead of being suppressed, the TM_{12} mode is removed out of the operating band by reducing the patch length in this design.

Equ. (1) shows that the patch length determines the resonance frequency of the TM_{12} mode which has little effect on the resonance frequency of the TM_{10} and TM_{20} modes. Therefore, as depicted in Fig. 3, the gain of Ant. 2 becomes smooth, while the bandwidth is kept nearly unchanged. Fig. 4(c) and Fig. 4(d) respectively present the current distribution and the radiation pattern of Ant. 2 at 39 GHz. After reducing the length of the patch, the TM_{12} mode is removed at 39 GHz, the radiation pattern is improved significantly and the gain is increased from 4.9 to 8.6 dBi. It should be noted that the length of the patch is reduced to be equal to the width of the patch in Ant. 2 which offers the possibility to achieve dual polarizations.

The proposed antenna is fed by two SICLs. To realize dual polarizations, the transverse slot is etched on the square patch as shown in Fig. 2. Similar to the longitudinal slot, the transverse slot changes the

Table 2. Performance Comparison of the Proposed Antenna and Those in References

Reference	Antenna configuration	Fabrication	Polarisation	Size (λ_0^3)	Frequency (GHz)	Imp. BW
[5]	Symmetrical E-shaped patch + SIW	PCB	Single	$0.46 \times 0.70 \times 0.08$	37.5	45.0%
[12]	Patch + SIW	PCB	Dual linear	$0.39 \times 0.39 \times 0.15$	28	14.0%
[15]	Stacked patch + Stripline	PCB	Dual linear	$0.53 \times 0.53 \times 0.15$	27	29.2%
[16]	ME dipole + L-probe	LTCC	Dual linear	$0.34 \times 0.34 \times 0.12$	33	42.5%
This work	Cross-slotted square patch + SICL	PCB	Dual linear	$0.38 \times 0.38 \times 0.19$	32	50.0%

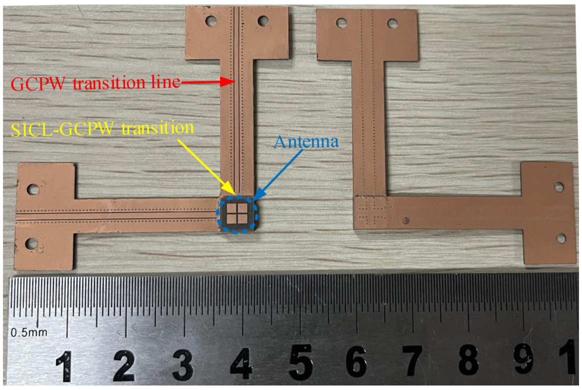

Fig 5 *Photograph of the top and bottom of the proposed antenna.*

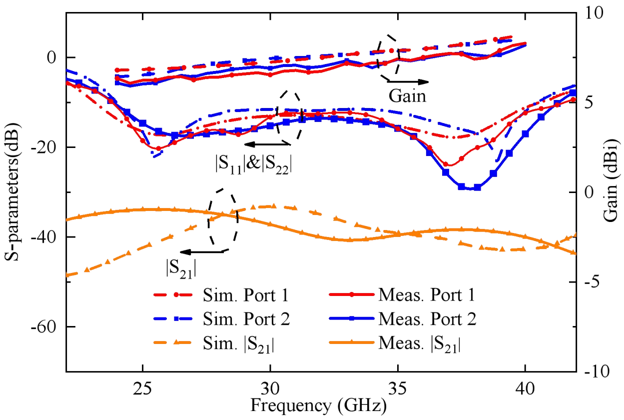

Fig 6 *Simulated and measured S-parameters and gains of the proposed antenna.*

E-field distribution of the TM_{02} mode which has a small effect on the E-field distribution of the TM_{01} mode. By combining the two modes, the H-polarisation is achieved. Importantly, as shown in Fig. 4(e), the transverse slot has little effect on the current distribution of the V-polarisation due to the direction of the transverse slot is parallel to the current direction of the V-polarisation. By combining the V-polarised radiation and the H-polarisation, a broadband dual-polarised patch antenna is achieved. The current distribution and the radiation pattern of these two polarisation are shown in Figs. 4(e)–4(h).

Results and Discussion:

Simulated and Measured Results: The photograph of the fabricated prototype is shown in Fig. 5. The ground coplanar waveguide (GCPW) transmission structure, the GCPW-SICL transition, and the Southwest End Launch Connector are utilized for the purpose of measurement. The connector size is more larger than the size of the proposed antenna. Therefore, to reduce the impact to radiation patterns, the connector should be placed far from the antenna. In the prototype, the length of the GCPW transition line is 35 mm. The simulated total loss of the GCPW transition line and the GCPW-SICL transition is less than 0.55 dB in the operating bandwidth.

The S-parameters and gains are shown in Fig. 6. The measured relative impedance bandwidth is greater than 50.0% for $|S_{11}| \leq -10$ dB and

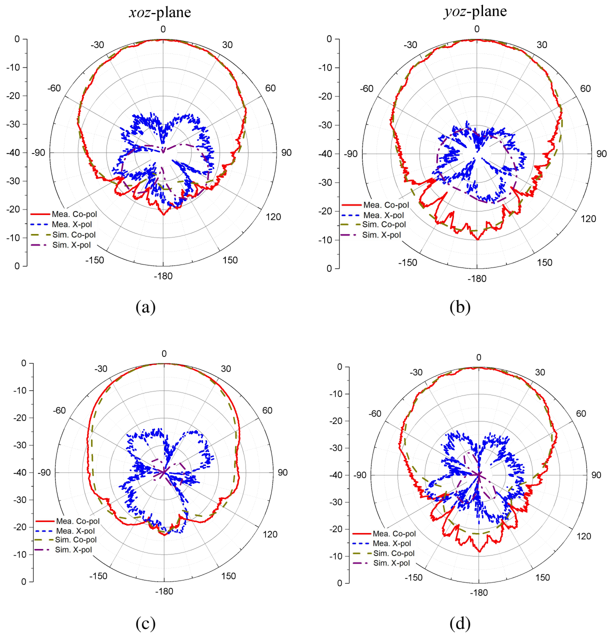

Fig 7 *Simulated and measured normalized radiation patterns of the proposed antenna when port 1 is excited. (a) At 26.0 GHz and in the* xoz*-plane; (b) At 26.0 GHz and in the* yoz*-plane; (c) At 38.0 GHz and in the* xoz*-plane; (d) At 38.0 GHz and in the* yoz*-plane.*

$|S_{22}| \leq -10$ dB. The gating method in time domain is used to smooth the measured S-parameters which can eliminate the ringing effect caused by the Southwest End Launch Connector and the GCPW transmission structure. The gain varies from 5.9 to 8.1 dBi over the operating frequency band when Port 1 is excited. Also, the gain varies from 6.0 to 8.1 dBi when Port 2 is excited.

The measured normalized radiation patterns of the proposed antenna in the *xoz* and *yoz* planes when port 1 is excited are shown in Fig. 7 and the simulated and measured co-polarizations strongly agree. The measured front-to-rear ratio is better than 10 dB. The cross-polarisation ratio is almost less than −20 dB. The measured cross-polarisation is deteriorated because of the influence of the metallic GCPW transmission line and the metallic launch. The similar radiation characteristics are achieved when port 2 is excited.

Comparison and Discussion: A performance comparison between the proposed SCSSP antenna and reported mmWave broadband antennas using different technologies is summarized in Table 2. The symmetrical E-shaped patch antenna [5] can also achieve wide impedance bandwidth, but it has only one polarisation and its length is greater than $0.5\lambda_0$. The antennas in [12, 15, 16] can realize dual polarisations, but the relative operating bandwidth of these antennas are less than 30% which cannot cover the candidate frequency bands from 24 GHz to 40 GHz. The length and width of the antenna in [15] are both greater than $0.5\lambda_0$. Although the ME dipole in [16] has dual polarisation and wide bandwidth, the LTCC fabrication is high-cost and difficult. Therefore, in terms of polarisation, bandwidth, structure, and fabrication cost, the proposed SCSSP antenna achieves significant improvement in comparison to the previous designs.

Conclusion: A multi-resonance broadband dual-polarised SCSSP antenna that is SICL-fed and aperture-coupled has been proposed. Two orthogonal slots are etched on the square patch to realize broadband broadside radiation patterns. Two SICLs are located in different layers, which can make high isolation between the two input ports. The proposed antenna achieves a ultra-wide bandwidth of 50% and a very high port isolation over 30 dB. Compared the previous designs, the proposed SCSSP antenna has realized considerable enhancement in terms of polarisation and bandwidth. Furthermore, the proposed SCSSP antenna with compact size, planar shape, and simple vertical feeding is very suitable for two-dimensional array design. The measured and simulated results agree very well, which validates the effectiveness of the proposed design. The proposed dual-polarised SCSSP antenna which covers both 26 GHz and 39 GHz bands is definitely a very attractive candidate for 5G mmWave broadband applications.

Acknowledgments: This work was supported in part by the National Natural Science Foundation of China under Grants 62271133 and 62001101, and the Science Foundation of Jiangsu Province of China under Grant BK20200349. The authors wish to thank the editors and anonymous reviewers for their valuable comments and suggestions. And the authors are also grateful to their colleagues in the State Key Laboratory of Millimeter Waves, Southeast University, Nanjing, China, for their valuable discussions and support in measurements.

Received: 25 November 2022 *Accepted:* 30 March 2023
doi: 10.1049/ell2.10001

References

1. Rappaport, T.S., et al.: Millimeter wave mobile communications for 5G cellular: It will work! IEEE Access 1, 335–349 (2013)
2. Results of the first session of the Conference Preparatory Meeting for WRC-19 (CPM19-1). document CA/226, ITU-R Administrative Circular (2015)
3. Jo, O., et al.: Exploitation of dual-polarization diversity for 5G millimeter-wave MIMO beamforming systems. IEEE Trans. Antennas Propag. 65(12), 6646–6655 (2017)
4. Fan, K., Hao, Z.C., Yuan, Q.: A low-profile wideband substrate-integrated waveguide cavity-backed E-shaped patch antenna for the Q-LINKPAN applications. IEEE Trans. Antennas Propag. 65(11), 5667–5676 (2017)
5. Yin, J., et al.: Broadband symmetrical E-shaped patch antenna with multimode resonance for 5G millimeter-wave applications. IEEE Trans. Antennas Propag. 67(7), 4474–4483 (2019)
6. Wu, Q., et al.: Broadband planar SIW cavity-backed slot antennas aided by unbalanced shorting vias. IEEE Antennas Wirel. Propag. Lett. 18(2), 363–367 (2019)
7. Dai, X., Li, A., Luk, K.M.: A wideband compact magnetoelectric dipole antenna fed by SICL for millimeter wave applications. IEEE Trans. Antennas Propag. 69(9), 5278–5285 (2021)
8. Sun, D., et al.: A broadband proximity-coupled stacked microstrip antenna with cavity-backed configuration. IEEE Antennas Wirel. Propag. Lett. 10, 1055–1058 (2011)
9. Wang, L., Guo, Y.X., Sheng, W.X.: Wideband high-gain 60-GHz LTCC L-probe patch antenna array with a soft surface. IEEE Trans. Antennas Propag. 61(4), 1802–1809 (2013)
10. Cheng, Y.F., et al.: Design and analysis of a bow-tie slot-coupled wideband metasurface antenna. IEEE Antennas Wirel. Propag. Lett. 18(7), 1342–1346 (2019)
11. Li, Y., Luk, K.M.: 60-GHz dual-polarized two-dimensional switch-beam wideband antenna array of aperture-coupled magneto-electric dipoles. IEEE Trans. Antennas Propag. 64(2), 554–563 (2016)
12. Yang, Q., et al.: Millimeter-wave dual-polarized differentially fed 2-D multibeam patch antenna array. IEEE Trans. Antennas Propag. 68(10), 7007–7016 (2020)
13. Liu, W., Yan, S.: A design of millimeter-wave dual-polarized siw phased array antenna using characteristic mode analysis. IEEE Antennas Wirel. Propag. Lett. 21(1), 29–33 (2022)
14. Dadgarpour, A., et al.: A dual-polarized magnetoelectric dipole array based on printed ridge gap waveguide with dual-polarized split-ring resonator lens. IEEE Trans. Antennas Propag. 68(5), 3578–3585 (2020)
15. Tong, X., et al.: Low-profile, broadband, dual-linearly polarized, and wide-angle millimeter-wave antenna arrays for Ka-band 5G applications. IEEE Antennas Wirel. Propag. Lett. 20(10), 2038–2042 (2021)
16. Li, Y., Wang, C., Guo, Y.X.: A Ka-band wideband dual-polarized magnetoelectric dipole antenna array on LTCC. IEEE Trans. Antennas Propag. 68(6), 4985–4990 (2020)
17. Yong, W.Y., et al.: A bandwidth-enhanced cavity-backed slot array antenna for mmwave fixed-beam applications. IEEE Antennas Wirel. Propag. Lett. 19(11), 1924–1928 (2020)
18. Balanis, C.A.: Antenna theory: analysis and design. John wiley & sons, USA (2015)